



Meta-STDP Rule Stabilizes Synaptic Weights Under *in Vivo*-like Ongoing Spontaneous Activity in a Computational Model of CA1 Pyramidal Cell

Matúš Tomko¹(✉), Peter Jedlička^{2,3}, and Ľubica Beňušková¹

- ¹ Centre for Cognitive Science, Department of Applied Informatics, Faculty of Mathematics, Physics and Informatics, Comenius University in Bratislava, Mlynská dolina, Bratislava, Slovakia
matus.tomko@fmph.uniba.sk
- ² Faculty of Medicine, ICAR3R - Interdisciplinary Centre for 3Rs in Animal Research, Justus-Liebig-University, Giessen, Germany
- ³ Frankfurt Institute for Advanced Studies, Frankfurt am Main, Germany

Abstract. It is widely accepted that in the brain processes related to learning and memory there are changes at the level of synapses. Synapses have the ability to change their strength depending on the stimuli, which is called activity-dependent synaptic plasticity. To date, many mathematical models describing activity-dependent synaptic plasticity have been introduced. However, the remaining question is whether these rules apply in general to the whole brain or only to individual areas or even just to individual types of cells. Here, we decided to test whether the well-known rule of Spike-Timing Dependent Plasticity (STDP) extended by metaplasticity (meta-STDP) supports long-term stability of major synaptic inputs to hippocampal CA1 pyramidal neurons. For this reason, we have coupled synaptic models equipped with a previously established meta-STDP rule to a biophysically realistic computational model of the hippocampal CA1 pyramidal cell with a simplified dendritic tree. Our simulations show that the meta-STDP rule is able to keep synaptic weights stable during ongoing spontaneous input activity as it happens in the hippocampus *in vivo*. This is functionally advantageous as neurons should not change their weights during the ongoing activity of neural circuits *in vivo*. However, they should maintain their ability to display plastic changes in the case of significantly different or “meaningful” inputs. Thus, our study is the first step before we attempt to simulate different stimulation protocols which induce changes in synaptic weights *in vivo*.

Keywords: Synaptic plasticity · Metaplasticity · Meta-STDP · Computational model · CA1 pyramidal cell

1 Introduction

Hippocampal CA1 pyramidal cells are crucially involved in processes associated with a learning and memory. That includes working memory [1–3], temporal processing of

information [4], and several others. CA1 pyramidal cells are the major excitatory cells of the CA1 region of hippocampus.

Synaptic plasticity is believed to be a key neural mechanism behind major types of memory. It represents the ability of neurons to strengthen and weaken synaptic weights or synaptic transmission depending on input/output activity. The most studied forms of long-term synaptic plasticity are long-term changes in synaptic weights referred to as long-term potentiation (LTP) and long-term depression (LTD) [5] as it is reviewed for instance in the paper of Martin et al. [6], which states: “activity-dependent synaptic plasticity is induced at appropriate synapses during memory formation and is both necessary and sufficient for the encoding and trace storage of the type of memory mediated by the brain area in which it is observed” [6].

So far, several models of synaptic plasticity have been introduced [7]. The meta-STDP rule of synaptic plasticity [8] used in our project is the nearest-neighbor implementation of the STDP rule [9], which is extended by metaplasticity [10]. The prefix “meta” points to the fact that synaptic plasticity itself is regulated by various mechanisms and thus manifests its higher-order character. One of the important factors of metaplasticity is the dependence of the outcome of synaptic plasticity upon the previous history of firing of the postsynaptic neuron [10]. This idea was used by Benuskova and Abraham [8] in modifying the classical STDP rule. Due to the use of metaplasticity, the amplitudes of LTP and LTD become dynamic and change their actual values depending on the previous postsynaptic activity [8]. The meta-STDP rule has already been successfully used in modeling studies of heterosynaptic plasticity in the hippocampal granule cells [8, 11]. Heterosynaptic plasticity means that stimulation of one input pathway leads to synaptic changes not only of the stimulated pathway (homosynaptic plasticity) but also of the neighboring unstimulated pathway, which receives only the spontaneous activity. The computational model of granule cell endowed with this meta-STDP rule was able to reproduce the experimental results of synaptic plasticity observed in these neurons. Among other things, ongoing spontaneous activity simulated in the model proved to be a key factor influencing the magnitude of homo-LTP and hetero-LTD. The phenomenon of spontaneous activity affecting the magnitude of synaptic changes was previously demonstrated experimentally by Abraham et al. [12]. As in hippocampal granule cells, homosynaptic and heterosynaptic plasticity has also been observed in CA1 pyramidal cells.

In this work, we applied the meta-STDP synaptic plasticity to a realistic compartmental model of CA1 pyramidal cell with reduced morphology. Our aim was to simulate the effects of ongoing spontaneous activity [13, 14] on the long-term stability of synaptic weights in the hippocampus. After optimization of model parameters and parameters of the meta-STDP rule, the result of this process was the achievement of dynamically stable synaptic weights.

2 Methods

2.1 Computational Model of CA1 Pyramidal Cell

In creating of our model, we were inspired by a previously published model from Cutsuridis et al. [15], which is available online in the ModeDB database under accession

No. 123815, and which we used in our previous study [16]. However, we have extended the morphology since this model did not contain the side dendritic branches where the majority of excitatory inputs is located in the real cell especially in the proximal and medial parts of the dendritic tree [17]. Basal dendrites in the stratum oriens (SO) were modeled by two thicker proximal sections, followed by 2 thinner distal sections. We added another 2 distal sections while maintaining the same parameters as the original distal sections. An apical trunk 400 μm long in the stratum radiatum (SR) consisted of 3 interconnected sections, which decreased in thickness with increasing distance from the soma. We attached one section to the center of each section of the apical trunk, representing thin oblique dendrites. A dendritic tuft in the stratum lacunosum-moleculare (SLM) was represented by two dendrites, each consisting of 3 sections with gradually decreasing thickness. We have kept this part unchanged [15]. The original model also contained an axon, which we also preserved. The structure of the model and typical somatic responses are shown in the Fig. 1.

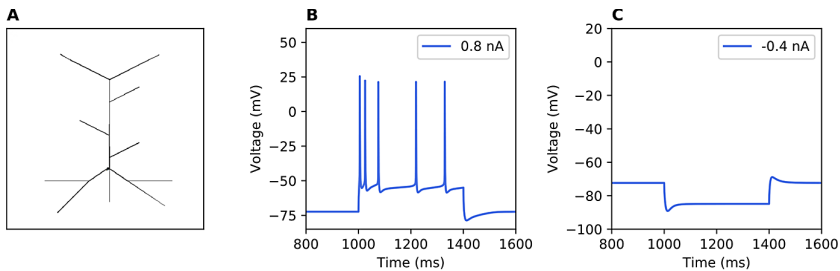


Fig. 1. Morphology and typical somatic responses of the model. (A) The reduced morphology of the model captures all essential parts of the dendritic tree of CA1 neurons. (B), (C) The typical somatic responses of the model to the positive and negative somatic current injections.

Passive and active properties of our model were adapted from the full-morphology model of CA1 pyramidal cell presented in the paper of the Migliore et al. [18] which is accessible in the ModelDB database (accession No. 244688). All apical and basal sections have uniformly distributed sodium current, a delayed rectifier K⁺ current (K_{dr}), a dendritic A-Type K⁺ current (K_A), a hyperpolarization-activated cation current (I_h), tree types of Ca²⁺ currents (Ca_L, Ca_N, Ca_T), and two types of calcium-activated K⁺ currents (K_{Ca} and Cagk). The somatic section has the same set of currents. However, a dendritic A-Type K⁺ current is exchanged for a somatic A-Type K⁺ current and a somatic M-Type K⁺ current (K_M) is included. The axonal section contains a sodium current, a delayed rectifier K⁺ current, and M-Type and A-Type K⁺ currents. Each section containing calcium current contains a simple calcium extrusion mechanism. The peak conductivity of I_h and K_A were calculated separately for each section according to its distance from the soma. Similarly, the equilibrium potential of the passive current (e_{pas}) was calculated for each section [18].

2.2 Model Synaptic Inputs

Excitatory synapses are modeled using NEURON [19] built-in synapse class *Exp2Syn*. Synaptic conductivity is expressed using a two-state kinetic scheme described by two exponential functions:

$$g(t) = w \left(e^{-\frac{t}{\tau_2}} - e^{-\frac{t}{\tau_1}} \right) \quad (1)$$

where w is the synaptic weight, $\tau_1 = 0.5$ ms is the rise time constant, and $\tau_2 = 3$ ms is the decay time constant [15]. The synaptic weight is modified according to the meta-STDP plasticity rule (see below).

Each synapse received a train of presynaptic spikes that were generated by independent spikes generators. In NEURON it is taken care of by the built-in process *NetStim*. Presynaptic spikes sequence delivered to one synapse consisted of a combination of random and periodic spike trains. We have chosen this strategy because we can thus simulate the theta activity that is a prominent state of the hippocampal network [20], plus the random spikes.

2.3 Synaptic Plasticity Rule

To model synaptic plasticity, we used the meta-STDP rule with the nearest neighbor implementation. In this implementation, each presynaptic spike is paired with two time-closest postsynaptic spikes. One occurring before the presynaptic spike and the other occurring after the presynaptic spike. The choice of this pairing scheme is related to the fact that it is biologically relevant, as it agrees with the Bienenstock-Cooper-Munro (BCM) theory [21] as shown by Izhikevich and Desai [22]. The weight change is calculated as:

$$w(t + \Delta t) = w(t)(1 + \Delta w_p - \Delta w_d) \quad (2)$$

where Δw_p is positive weight change and Δw_d is negative weight change.

The positive weight change (potentiation) occurs when the presynaptic spike precedes the postsynaptic spike. On the other hand, weakening of the weight (depression) occurs when the postsynaptic spike precedes the presynaptic spike. It is formulated as:

$$\Delta w_p(\Delta t) = A_p \exp\left(-\frac{\Delta t}{\tau_p}\right) \Delta t > 0 \quad (3)$$

$$\Delta w_d(\Delta t) = A_d \exp\left(\frac{\Delta t}{\tau_d}\right) \text{ if } \Delta t < 0 \quad (4)$$

where $\Delta t = t_{post} - t_{pre}$, A_p and A_d are potentiation and depression amplitudes, respectively, τ_p and τ_d are decay constants for the time windows over which synaptic change can occur. Parameter t_{post} represents the instant of time at which the local voltage on the postsynaptic dendrite, where a synapse is located, exceeds the threshold of -30 mV.

Amplitudes of LTP/LTD in the meta-STDP are dynamically changed as a function of a previous temporal average of soma spiking θ_S :

$$A_p(t) = A_p(0) \left(\frac{1}{\theta_S(t)} \right) \quad (5)$$

$$A_d(t) = A_d(0)\theta_S(t) \quad (6)$$

$$\theta_S(t) = \alpha \langle c \rangle_\tau = \frac{\alpha}{\tau} \int_{-\infty}^t c(t') \exp\left(\frac{-(t-t')}{\tau}\right) dt' \quad (7)$$

where $A_p(t)$ and $A_d(t)$ are amplitudes for potentiation and depression at time t , and α is a scaling constant. $A_p(0)$ and $A_d(0)$ are initial values at time 0. The term $\langle c \rangle_\tau$ expresses the weighted temporal average of the postsynaptic spike count, with the most recent spikes entering the sum with bigger weight than the previous ones [8]. The source code of *Exp2Syn* endowed with the meta-STDP rule is available on ModelDB database under accession number 185350. The simulations were performed with the NEURON simulation environment (version 7.7.2) [19] embedded in Python 2.7.16.

3 Results

When stabilizing the model, we worked with parameters from two groups. On the one hand, it was the number of synapses, the distribution of synapses on the dendrites and their initial weight values. The second group were the parameters of synaptic plasticity and metaplasticity. We analyzed the simulation results from both perspectives at the same time, but we always modified only one selected parameter. All these parameters were optimized by trial and error.

3.1 Number of Synapses, Distribution of Synapses and Initial Weights

We started with an initial number of synapses of 600, which we uniformly randomly distributed to the dendritic tree, maintaining the ratio of synapses on the individual branch parts according to Table 3 from the paper of Megías et al. [17]. The total number of excitatory synapses impinging on a single CA1 neuron was estimated to be about 30 000. Their relative representation on individual parts of the dendritic tree is as follows: 38.3% on the stratum oriens distal dendrites, 0.8% on the stratum oriens proximal dendrites, 0.9% on the stratum radiatum thick medial dendrites, 7.1% on the stratum radiatum thick distal dendrites, 47.1% on the stratum radiatum thin dendrites, 1.6% on the stratum lacunosum-moleculare thick dendrites, 1.4% on the stratum lacunosum-moleculare medial dendrites, and 2.8% on the stratum lacunosum-moleculare thin dendrites [17]. The number of synapses in individual layers were: stratum oriens – 240 (40%), stratum radiatum – 330 (55%), and stratum lacunosum-moleculare – 30 (5%).

The meta-STDP synaptic plasticity rule requires the model cell to fire as is the case *in vivo*. Our goal was to achieve an output firing frequency of about 2 Hz, which was also observed *in vivo* [23]. We decided to generate the initial synaptic weights from the normal distribution, while we experimentally found suitable parameters of the normal distribution, namely $\mu = 0.000165$ and $\sigma = 0.000015$. For any randomly generated initial synaptic weights from the normal distribution thus defined, the meta-STDP rule ensured that the synaptic weights were dynamically stable during ongoing spontaneous activity and at the same time the output frequency was around 2 Hz. This

result is important because even in *in vivo* experiments, the stable baseline is measured for some time before applying the stimulation protocol [12]. We also experimented with the lognormal distribution of initial weights, which was observed in several *in vitro*, *-ex vivo*, and *in vivo* studies [24]. Our unpublished results suggest that the meta-STDP rule is able to maintain dynamically stable weights generated from the lognormal distribution.

When generating weights from the normal distribution with the indicated parameters and simulating spontaneous activity for 20 min, 3 groups of synapses were formed at the end of the simulation. The first group consisted of synapses, the final weights of which were more or less the same as the initial ones (change in weights $\pm 5\%$). The second group consisted of synapses that were attenuated, and their final weights were approximately 50% lower than the initial ones. The last group consisted of synapses with weight changes between 5–50%. It should be noted here that in each group there were synapses with different initial weights and from different parts of the dendritic tree. At this point, we asked ourselves the question of whether synapses, whose weights have significantly decreased as a result of spontaneous activity, are necessary to stabilize the entire system. We decided to remove them, reducing the total number of synapses to 391. Thus, the resulting number of synapses in individual layers is as follows: stratum oriens – 158 (40.4%), stratum radiatum – 203 (51.9%), and stratum lacunosum-moleculare – 30 (7.6%) As we can see from the results, the percentage of synapses within each layer was maintained as in [17]. Due to the removal of synapses, we increased all initial weights by 20% in order to maintain cell firing which is necessary to activate synaptic plasticity and metaplasticity in our meta-STDP rule.

3.2 Synaptic Plasticity Parameters

In evaluating the stability of synaptic plasticity and metaplasticity parameters, we monitor the evolution of depression and potentiation amplitudes and the evolution of the integrated spike count scaled by alpha over time (Eq. 7). The integrated spike count is important because the amplitudes are adjusted based on it. This mechanism represents metaplasticity. In simulations, it is crucial that its value oscillates around the value 1. Values higher than one results in increased depression and weakened potentiation. Conversely, values less than one yield potentiation to be attenuated and depression enhanced. Slight oscillations around 1 will ensure dynamically stable amplitudes and thus the entire system. The free parameters are mainly alpha and the average time constant τ for the postsynaptic spike count (Eq. 7). The following proved to be the most suitable parameter values: $A_p(0) = 0.0001$, $A_d(0) = 0.0003$, $\tau_p = 20$ ms, $\tau_d = 20$ ms, $\tau = 100000$ ms, and $\alpha = 500$. The following figures show the results of potentiation and depression amplitudes (Fig. 2) and integrated spike count θ_S scaled by alpha (Fig. 3) for any typical simulation.

3.3 Results of Simulations

After simulating spontaneous activity for 20 min, we achieved dynamically stable synaptic weights in all layers. The figures (Fig. 4, 5, 6 and 7) show the results for any simulation with the best parameters of the meta-STDP plasticity rule for the period of 20 min.

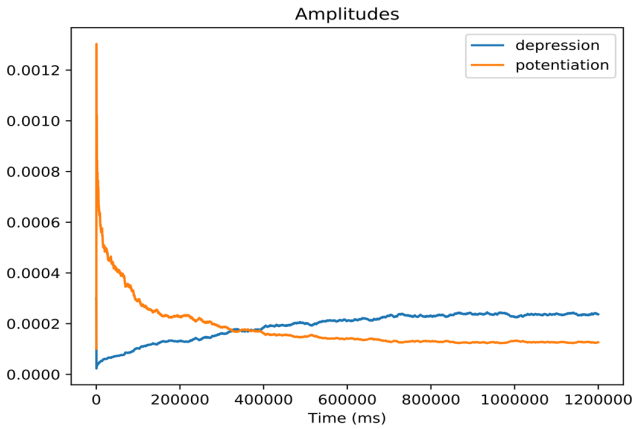


Fig. 2. The CA1 pyramidal cell model depression and potentiation amplitudes were stabilized after a short transitory period with employed meta-STDP rule.

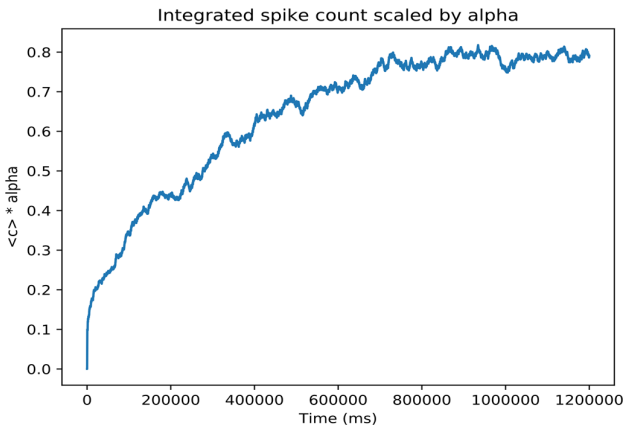


Fig. 3. Evolution of the integrated spike count scaled by alpha with employed meta-STDP rule applied to the synapses of the CA1 pyramidal cell model.

The results document that the weights are stable on average in all layers of the dendritic tree of the CA1 pyramidal cell model endowed with the meta-STDP synaptic plasticity rule.

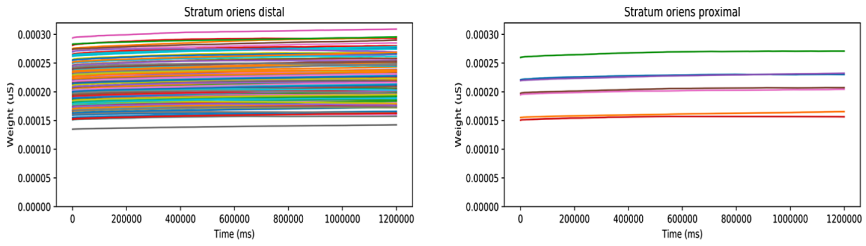


Fig. 4. Evolution of synaptic weights in the distal stratum oriens (left) and the proximal stratum oriens (right) of the CA1 pyramidal cell model. The x-axis denotes time in ms and the y-axis denotes values of synaptic weights.

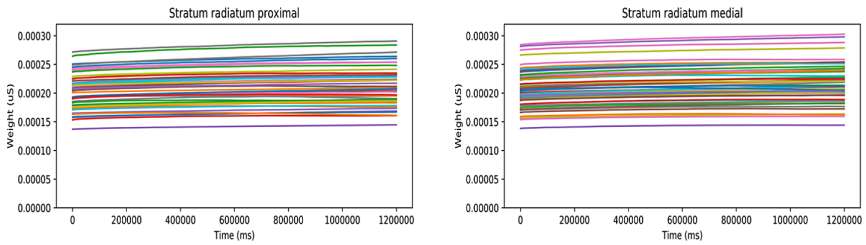


Fig. 5. Evolution of synaptic weights in the proximal stratum radiatum (left) and the medial stratum radiatum (right) of the CA1 pyramidal cell model. The x-axis denotes time in ms and the y-axis denotes values of synaptic weights.

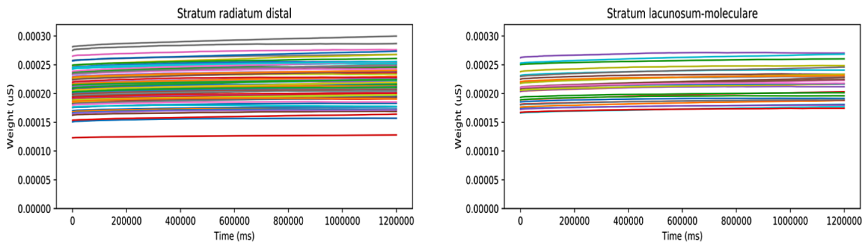


Fig. 6. Evolution of synaptic weights in the distal stratum radiatum (left) and the stratum lacunosum moleculare (right) of the CA1 pyramidal cell model. The x-axis denotes time in ms and the y-axis denotes values of synaptic weights.

4 Discussion

Computational studies that model synaptic plasticity *in vivo* neglect the fact that *in vivo* neurons exhibit an ongoing spontaneous spiking in the neural circuits [14]. The first synaptic plasticity theory that explicitly took into account ongoing neuronal activity was the BCM theory [21]. A key element of this BCM theory is a whole-cell variable termed the modification threshold, the tipping point at which the presynaptic activity either leads to long-term depression (LTD) or long-term potentiation (LTP) of synaptic efficacy. A second key element is the theory's postulate that the average ongoing level of

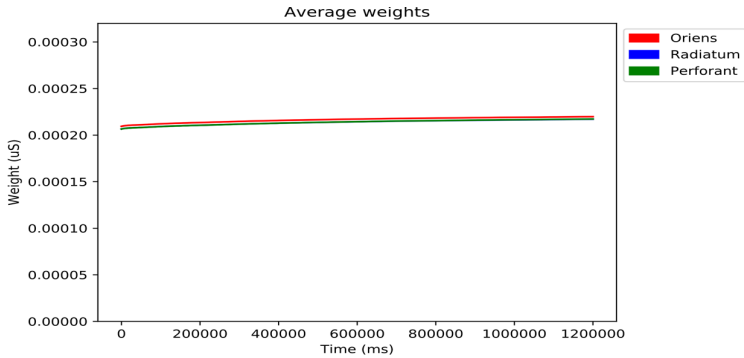


Fig. 7. Evolution of synaptic weights average in the stratum oriens, radiatum, and lacunosum-moleculare of the CA1 pyramidal cell model. The x-axis denotes time in ms and the y-axis denotes values of average synaptic weights.

spontaneous activity dynamically sets the position of the LTD/LTP tipping point in such a way that potentiation is favored when the postsynaptic cell firing is low on average and, vice versa, depression is favored when the postsynaptic activity is high on average. The BCM model has been used to account for experimental findings of experience-evoked plasticity in the developing visual [21] and adult somatosensory cortices *in vivo* [25]. The proposal of a modifiable plasticity threshold foreshadowed the concept of metaplasticity [10], developed to account for the abundant experimental evidence that prior neural activity can change the state of neurons and synapses such that the outcome of future synaptic plasticity protocols is altered.

Here we study how key components of learning mechanisms in the brain, namely spike timing-dependent plasticity and metaplasticity, interact with spontaneous activity in the input pathways of the CA1 neuron model.

In this study we optimized the synaptic model parameters to achieve the long-term stability of synaptic weights under *in vivo*-like conditions mimicking ongoing spontaneous activity as recorded in neuronal circuits [20]. Each synapse received an independent spike train input consisting of periodic spikes corresponding to theta activity and random spikes corresponding to random background activity. Average frequency of spikes in the one spike train was ~ 8 Hz. During the 20-min simulation of spontaneous activity, the individual synaptic weights and synaptic plasticity parameters are dynamically stable. These results provide a good basis for experimenting with synaptic plasticity stimulation protocols and ultimately for modeling the synaptic plasticity observed in CA1 pyramidal cells *in vivo*.

In our previous study [16], we used a model from Cutsuridis et al. [15]. Using HippoUnit tests [26], we tested and compared the latter model and our currently used model. As a result, our model achieved better results than the Cutsuridis model [15], which is more excitable (data not shown/paper in preparation). The consequence of the higher excitability of the Cutsuridis model was that at the beginning of each simulation there was a significant increase in the integrated spike count function θ_S and at the same time a decrease in the weights [16]. In our current model, the weights are dynamically stable from the beginning of the simulation (Fig. 4, 5, 6 and 7) and the integrated spike

count function θ_S saturation occurs gradually (Fig. 3). By adding side branches, we have ensured that experimentally observed non-linear summation of synaptic inputs occurs on these branches, resulting in dendritic spikes.

In summary, we have modified existing compartmental model of the CA1 pyramidal cell by adding the side dendrites, synapses, and by implementing synaptic plasticity rule, namely the meta-STDP rule. Our model exhibits realistic input-output spontaneous activity as neurons *in vivo*. During ongoing spontaneous activity, synapses should not change their weights. This has been achieved after manual optimization of synaptic model parameters. Next, we intend to implement several of synaptic plasticity protocols which were experimentally studied for CA1 pyramidal cells.

References

1. Lee, I., Jerman, T., Kesner, R.: Disruption of delayed memory for a sequence of spatial locations following CA1- or CA3-lesions of the dorsal hippocampus. *Neurobiol. Learn. Mem.* **84**, 138–147 (2005). <https://doi.org/10.1016/j.nlm.2005.06.002>
2. Lee, I., Kesner, R.P.: Differential contribution of NMDA receptors in hippocampal subregions to spatial working memory. *Nat. Neurosci.* **5**, 162–168 (2002). <https://doi.org/10.1038/nn790>
3. Lee, I., Kesner, R.P.: Differential contributions of dorsal hippocampal subregions to memory acquisition and retrieval in contextual fear-conditioning. *Hippocampus.* **14**, 301–310 (2004). <https://doi.org/10.1002/hipo.10177>
4. Hoang, L.T., Kesner, R.P.: Dorsal hippocampus, CA3, and CA1 lesions disrupt temporal sequence completion. *Behav. Neurosci.* **122**, 9–15 (2008). <https://doi.org/10.1037/0735-7044.122.1.9>
5. Hughes, J.R.: Post-tetanic potentiation. *Physiol. Rev.* **38**, 91–113 (1958). <https://doi.org/10.1152/physrev.1958.38.1.91>
6. Martin, S.J., Grimwood, P.D., Morris, R.G.M.: Synaptic plasticity and memory: an evaluation of the hypothesis. *Annu. Rev. Neurosci.* **23**, 649–711 (2000). <https://doi.org/10.1146/annurev.neuro.23.1.649>
7. Mayr, C.G., Partzsch, J.: Rate and pulse based plasticity governed by local synaptic state variables. *Front. Synaptic Neurosci.* **2**, 33 (2010). <https://doi.org/10.3389/fnsyn.2010.00033>
8. Benuskova, L., Abraham, W.C.: STDP rule endowed with the BCM sliding threshold accounts for hippocampal heterosynaptic plasticity. *J. Comput. Neurosci.* **22**, 129–133 (2007). <https://doi.org/10.1007/s10827-006-0002-x>
9. Markram, H., Lübke, J., Frotscher, M., Sakmann, B.: Regulation of synaptic efficacy by coincidence of postsynaptic APs and EPSPs. *Science* **275**, 213 (1997). <https://doi.org/10.1126/science.275.5297.213>
10. Abraham, W.C.: Metaplasticity: tuning synapses and networks for plasticity. *Nat. Rev. Neurosci.* **9**, 387 (2008). <https://doi.org/10.1038/nrn2356>
11. Jedlicka, P., Benuskova, L., Abraham, W.C.: A voltage-based STDP rule combined with fast BCM-Like metaplasticity accounts for LTP and concurrent “heterosynaptic” LTD in the dentate gyrus *in vivo*. *PLoS Comput. Biol.* **11**, e1004588–e1004588 (2015). <https://doi.org/10.1371/journal.pcbi.1004588>
12. Abraham, W.C., Logan, B., Wolff, A., Benuskova, L.: “Heterosynaptic” LTD in the dentate gyrus of anesthetized rat requires homosynaptic activity. *J. Neurophysiol.* **98**, 1048–1051 (2007). <https://doi.org/10.1152/jn.00250.2007>
13. Frank, L.M., Brown, E.N., Wilson, M.A.: A comparison of the firing properties of putative excitatory and inhibitory neurons from CA1 and the entorhinal cortex. *J. Neurophysiol.* **86**, 2029–2040 (2001). <https://doi.org/10.1152/jn.2001.86.4.2029>

14. Deshmukh, S.S., Yoganarasimha, D., Voicu, H., Knierim, J.J.: Theta modulation in the medial and the lateral entorhinal cortices. *J. Neurophysiol.* **104**, 994–1006 (2010). <https://doi.org/10.1152/jn.01141.2009>
15. Cutsuridis, V., Cobb, S., Graham, B.P.: Encoding and retrieval in a model of the hippocampal CA1 microcircuit. *Hippocampus* **20**, 423–446 (2010). <https://doi.org/10.1002/hipo.20661>
16. Tomko, M., Jedlička, P., Beňušková, Ľ.: Computational model of CA1 pyramidal cell with meta-STDP stabilizes under ongoing spontaneous activity as in vivo. In: *Kognícia a umelý život 2019*. Vydavateľstvo Univerzity Komenského, Bratislava (2019)
17. Megias, M., Emri, Z., Freund, T.F., Gulyás, A.I.: Total number and distribution of inhibitory and excitatory synapses on hippocampal CA1 pyramidal cells. *Neuroscience* **102**, 527–540 (2001). [https://doi.org/10.1016/S0306-4522\(00\)00496-6](https://doi.org/10.1016/S0306-4522(00)00496-6)
18. Migliore, R., et al.: The physiological variability of channel density in hippocampal CA1 pyramidal cells and interneurons explored using a unified data-driven modeling workflow. *PLoS Comput. Biol.* **14**, e1006423–e1006423 (2018). <https://doi.org/10.1371/journal.pcbi.1006423>
19. Hines, M.L., Carnevale, N.T.: The NEURON Simulation Environment. *Neural Comput.* **9**, 1179–1209 (1997). <https://doi.org/10.1162/neco.1997.9.6.1179>
20. Buzsáki, G.: Theta oscillations in the hippocampus. *Neuron* **33**, 325–340 (2002). [https://doi.org/10.1016/S0896-6273\(02\)00586-X](https://doi.org/10.1016/S0896-6273(02)00586-X)
21. Bienenstock, E.L., Cooper, L.N., Munro, P.W.: Theory for the development of neuron selectivity: orientation specificity and binocular interaction in visual cortex. *J. Neurosci. Off. J. Soc. Neurosci.* **2**, 32–48 (1982). <https://doi.org/10.1523/JNEUROSCI.02-01-00032.1982>
22. Izhikevich, E.M., Desai, N.S.: Relating STDP to BCM. *Neural Comput.* **15**, 1511–1523 (2003). <https://doi.org/10.1162/089976603321891783>
23. Mizuseki, K., Buzsáki, G.: Preconfigured, skewed distribution of firing rates in the hippocampus and entorhinal cortex. *Cell Rep.* **4**, 1010–1021 (2013). <https://doi.org/10.1016/j.celrep.2013.07.039>
24. Buzsáki, G., Mizuseki, K.: The log-dynamic brain: how skewed distributions affect network operations. *Nat. Rev. Neurosci.* **15**, 264–278 (2014). <https://doi.org/10.1038/nrn3687>
25. Benusková, L., Diamond, M.E., Ebner, F.F.: Dynamic synaptic modification threshold: computational model of experience-dependent plasticity in adult rat barrel cortex. *Proc. Natl. Acad. Sci. U. S. A.* **91**, 4791–4795 (1994). <https://doi.org/10.1073/pnas.91.11.4791>
26. Sáray, S., et al.: Systematic comparison and automated validation of detailed models of hippocampal neurons. *bioRxiv*. 2020.07.02.184333 (2020). <https://doi.org/10.1101/2020.07.02.184333>